Rare Metal Materials and Engineering
Volume 47, Issue 10, October 2018
Online English edition of the Chinese language journal

Available online at www.sciencedirect.com
ScienceDirect

Cite this article as: Rare Metal Materials and Engineering, 2018, 47(10): 2964-2969.

ARTICLE

Transverse Tensile Properties of a Nickel-based Third Generation Single Crystal Superalloy

Yang Wanpeng, Li Jiarong, Liu Shizhong, Shi Zhenxue, Zhao Jinqian, Wang Xiaoguang

Science and Technology on Advanced High Temperature Structural Materials Laboratory, Beijing Institute of Aeronautical Materials, Beijing 100095, China

Abstract: In the temperature range of 760 °C to 1100 °C, the transverse tensile properties of a nickel-based third generation single crystal superalloy were studied. The microstructures and fracture surfaces were observed by optical microscopy (OM), field emission scanning electron microscopy (FESEM) and scanning transmission electron microscopy (STEM). The results show that the tensile strength of the alloy decreases as the temperature increases, while the tensile elongation of the alloy increases with the temperature increasing. The fracture surfaces of the tensile ruptured specimens are characterized by quasi-cleavage features at 760 and 850 °C. In the temperature range of 980 °C to 1100 °C, dendrites characteristics exhibiting the solidification direction are observed on the fracture surfaces and the proportion of dendrites characteristic on the fracture surfaces increases with the temperature increasing. The fracture surface displays mixed quasi-cleavage and dimple features at 980 °C. The fracture surfaces are characterized by dimples at 1070 and 1100 °C. As the temperature increases, more slip systems tend to be activated during the plastic deformation, resulting in different dislocation configurations. At 760°C, high density $a/2<110>$ dislocations are found to be of a roughly parallel distribution with each other in the tensile ruptured specimens. The dislocations are observed to be tangled at 980 °C and dislocation networks have formed at 1100 °C.

Key words: third generation single crystal superalloy; transverse tensile properties; fracture surface; dislocation

Nickel-based single crystal superalloys have been widely used as turbine blade materials in advanced aero gas turbine engines due to their excellent comprehensive properties[1-3]. Single crystal turbine blades in advanced aero engines have to withstand critical conditions in terms of high service temperatures and stresses, and the load axis is usually parallel to [001] orientation of the single crystal turbine blade. However, the stress state in the rabbet is complex, and the rabbet would sustain tensile stress which is perpendicular to the [001] orientation. Moreover, the solidification behavior of single crystal superalloys determines that their microstructures are composed of dendritic cores and interdendritic regions. The strength difference between the dendritic arms and interdendritic regions can lead to the difference of transverse and longitudinal properties of single crystal superalloy. Although researches of the tensile properties of single crystal superalloys mainly focus on the [001] orientation[4-8], transverse tensile properties are still one of the important research aspects of the single crystal superalloys.

There are a few reports on the transverse tensile properties of the single crystal superalloys in the open literature. The transverse tensile properties of the second generation single crystal superalloy DD6 have been investigated[9,10]. The primary goal of this paper is to report the transverse tensile properties and fracture behavior of a third generation single crystal superalloy in the temperature range of 760 °C to 1100 °C.

1 Experiment

The master alloy was melted in a vacuum induction furnace with commercially pure raw materials. The chemical

Received date: October 25, 2017
Corresponding author: Yang Wanpeng, Candidate for Ph. D., Science and Technology on Advanced High Temperature Structural Materials Laboratory, Beijing Institute of Aeronautical Materials, Beijing 100095, P. R. China, Tel: 0086-10-62498312, E-mail: wp_yang621@126.com

compositions (wt%) of the alloy is: Cr 1.5~5.0, Co 5.5~9.5, Mo 0.5~3.0, W 6.0~8.5, Al 5.2~6.2, Ta 5.5~9.0, Re 3.5~5.0, Hf 0~0.5, Nb 0~1.5, C 0~0.04, Ni balance. Single crystal superalloy slabs with dimensions of 15 mm × 80 mm × 120 mm were cast in a directional solidification vacuum furnace using a seed crystal method. The growth direction of the seed was [001] orientation. The orientations of the single crystal slabs were determined with X-ray technology, and the slab with [001] orientation deviating from the longitudinal direction within 10° was chosen. The schematic of the single crystal slab and the transverse specimen is shown in Fig.1.

The transverse specimens were heat treated according to the following heat treatment regime: pre-heat treatment + 1340 °C/6 h AC + 1120 °C/4 h AC + 870 °C/32 h AC. The specimens were machined into the standard tensile test ones after the heat treatment. The tensile test was performed at 760 , 850, 980, 1070 and 1100 °C. The fracture surfaces of ruptured specimens were examined by SUPRA 55 field emission scanning electron microscopy (FESEM). The ruptured specimens were then cut along the section parallel to the tensile axis, and the microstructures of the sections were observed by optical microscopy (OM), SUPRA 55 field emission scanning electron microscopy (FESEM) and JEOL JEM-2100F field emission scanning transmission electron microscopy (STEM).

2 Results and Discussion

2.1 Transverse tensile properties

Table 1 lists the transverse tensile properties of the alloy at 760, 850 980, 1070 and 1100 °C. Relationships between the transverse tensile properties of the alloy and temperatures are shown in Fig.2. The error bars denote their standard deviation. The results show that the yield strength (YS) of the alloy decreases as the temperature increases, and it decreases faster when the temperature is above 980 °C. The ultimate tensile strength (UTS) of the alloy decreases as the temperature increases in the temperature range of 850 °C to 1100 °C. However, the elongation of the alloy increases with the temperature increasing, and the elongations at 1070 and 1100 °C are almost the same. That is to say, the transverse tensile strength is the highest and the transverse tensile elongation is relatively low at the medium temperature. With the increasing of temperature, the transverse tensile strength becomes lower and the transverse tensile elongation becomes higher.

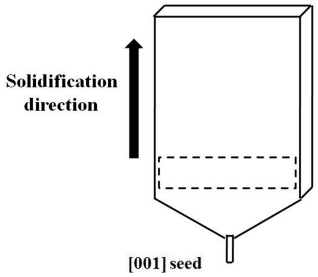

Fig.1 Schematic of the single crystal slab and transverse specimen

Table 1 Transverse tensile properties of the alloy at different temperatures

Temperature/°C	YS/MPa	UTS/MPa	δ_5/%
760	840	978	9.4
850	822	1006	14.8
980	802	845	22.5
1070	550	609	29.3
1100	472	532	29.8

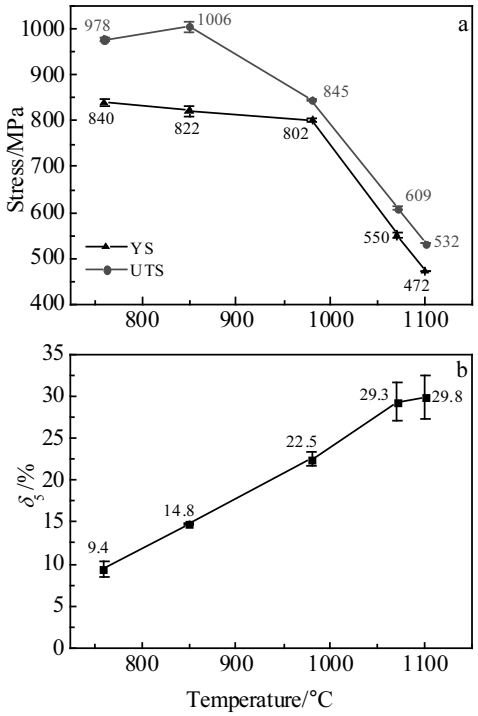

Fig.2 Relationships between the transverse tensile properties of the alloy and temperatures: (a) yield strength and ultimate tensile strength and (b) elongation

2.2 Transverse tensile fracture

Fig.3 shows the tensile fracture surfaces and longitudinal photographs of the transverse specimens of the alloy. At 760 °C, the fracture surface is almost a single elliptical plane, and there are river patterns on the fracture surface (Fig.3a). The neck-down of the specimen is not obvious near the fracture surface (Fig.3b). The fracture surface at 850 °C is composed of many small planes with tear ridges between them (Fig.3c), and a slight neck-down of the specimen can be observed near the fracture surface (Fig.3d). The fracture surfaces at 760 and 850 °C are both characterized by quasi-cleavage features. Fig.4 shows a higher magnification of the longitudinal surface at 760 and 850 °C. It can be seen that there are slip bands parallel to the fracture surface at 760 °C, as indicated by arrows in Fig.4a. At 850 °C, at least two slip bands along different

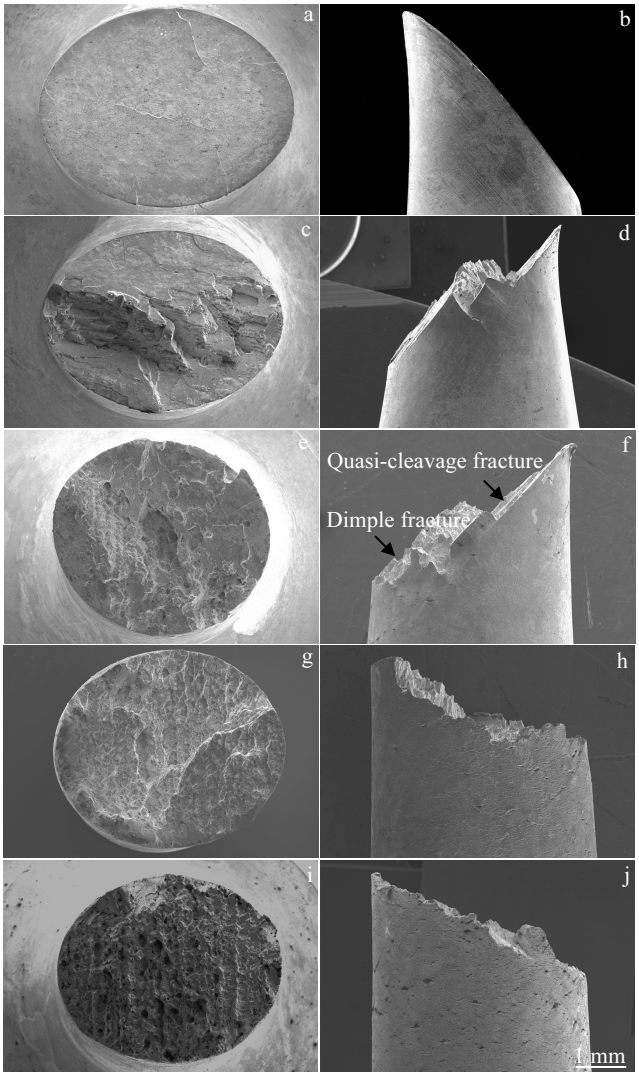

Fig.3 Transverse tensile fracture surface and longitudinal morphologies of the alloy at 760 °C (a, b), 850 °C (c, d), 980 °C (e, f), 1070 °C (g, h) and 1100 °C (i, j)

directions near the fracture surface can be found, as indicated by arrows in Fig.4b, and correspondingly, the stage-like fracture surface appears.

At the temperatures of 980 °C, 1070 °C and 1100 °C, the fracture surfaces are circular and there is no apparent neck-down of the specimens near the fracture surface. At 980 °C, about half of the fracture surface is a single plane, and a small amount of dendrites characteristic and dimple features can be found on the other half of the fracture surface (Fig.3e). The fracture surface displays mixed quasi-cleavage and dimple features at 980 °C, as illustrated in Fig.3f. At 1070 °C and 1100 °C, dendrites characteristic and dimple features can be observed on both the fracture surfaces, and the proportion of dendrites characteristic on the fracture surface at 1100 °C is apparently more than that at 1070 °C (Fig.3g and Fig.3i). At a

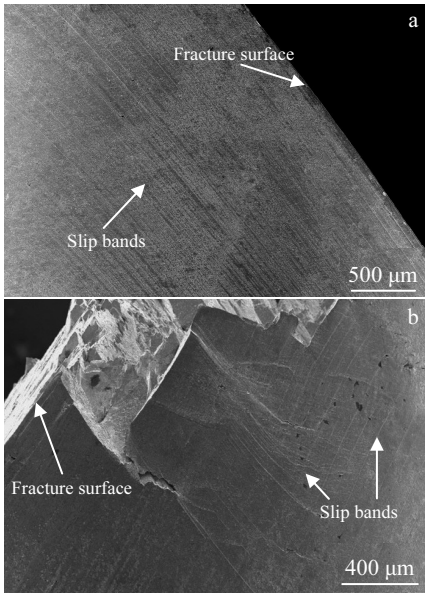

Fig.4 Slip bands on the surface of the tensile ruptured specimen at 760 °C (a) and 850 °C (b)

higher magnification, it is found that there is almost one small pore in the center of each dimple, as shown in Fig.5. Many microcracks on the longitudinal surface of the specimen can be observed at 1070 °C and 1100 °C (Fig.3h and Fig.3j). The fracture surfaces at 1070 °C and 1100 °C are characterized by dimple features.

2.3 Microstructures of the specimens after tensile fracture

Fig.6 illustrates the morphologies of the longitudinal section of transverse tensile ruptured specimens at 760, 980 and 1100 °C. At 760 °C, no microcrack can be found on the longitudinal section. However, microcracks are observed on the longitudinal section at 980 and 1100 °C. As seen in Fig.6b and Fig.6c, it is obvious that there are more microcracks on the longitudinal section at 1100 °C than at 980 °C. Therefore, it can be concluded that as the temperature becomes higher, the quantities of microcracks on the surface and inside of the tensile ruptured specimens both increase, as seen in Fig.3 and Fig.6.

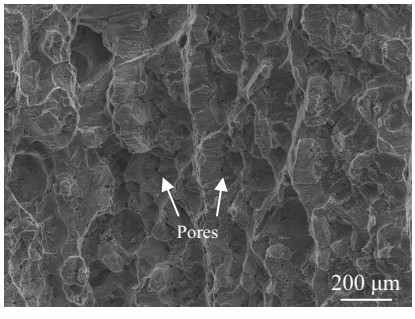

Fig.5 Dimples on the fracture surface of the tensile ruptured specimen at 1070 °C

Fig.7 illustrates the microstructures of the longitudinal sections of tensile ruptured specimens at 760, 980 and 1100 °C. Slip bands can be observed at all the three temperatures, as indicated by arrows in Fig.7. At 760 °C, some of the γ' phases get truncated by the slip bands and the cubic shape of them is not perfect, while the γ' phases in other parts remain cubic (Fig.7a). Meanwhile, it can be found that a crack propagates along the direction of the slip bands at 980 °C and there is a microcavity near the slip bands at 1100 °C, as shown in Fig.7b and Fig.7c.

Fig.8 shows STEM images of the microstructures of the longitudinal sections near fracture surface of tensile ruptured specimens at 760, 980 and 1100 °C. It can be seen that there are high density *a*/2<110> dislocations at 760 °C, which are of a roughly parallel distributing with each other (Fig.8a). These parallel dislocations belong to the same slip system, which indicates that the deformation mechanism of the alloy at 760 °C is mainly single slip. However, the dislocation configuration of the alloy tested at 980 °C is significantly different from that at 760 °C. The dislocations are observed to be tangled at 980 °C, which means the occurrence of multiple slip (Fig.8b). Moreover, it can be noted that dislocation networks have formed through dislocation reaction between different slip systems at 1100 °C (Fig.8c). As the temperature

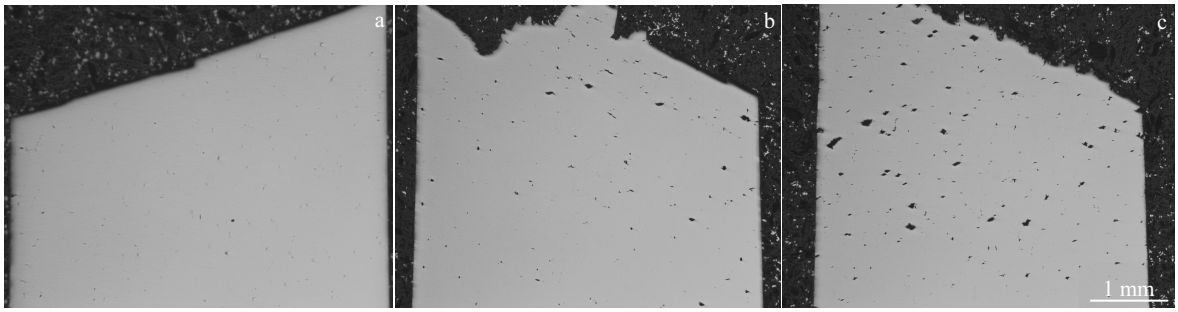

Fig.6 Morphologies of the longitudinal section of the tensile ruptured specimens at 760 °C (a), 980 °C (b) and 1100 °C (c)

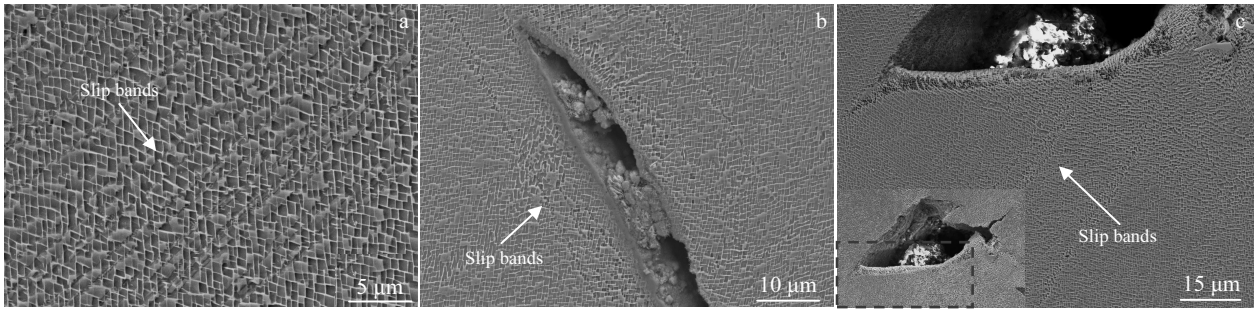

Fig.7 Microstructures of the longitudinal sections near fracture surface of tensile ruptured specimens at 760 °C (a), 980 °C (b) and 1100 °C (c)

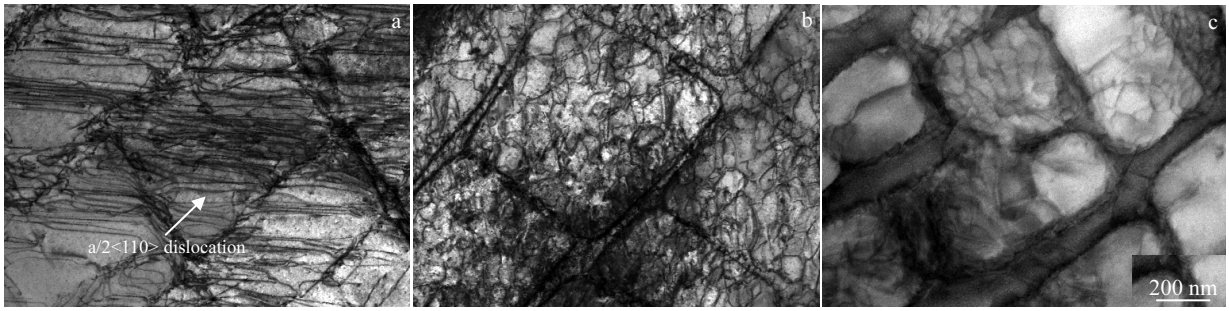

Fig.8 STEM images of the microstructures of the longitudinal sections near fracture surface of tensile ruptured specimens at 760 °C (a), 980 °C (b) and 1100 °C (c)

becomes higher, the activation energy need for initiating the slip systems decreases. Consequently, more slip systems are activated at high temperatures, including the octahedral slip and the hexahedral slip[11, 12]. In nickel-based single crystal superalloys, there are twelve octahedral primary slip systems {111}<110> and six hexahedral slip systems {001}<110>, both the slip directions of them are <110> direction and the slip planes of these two kinds of slip systems are {111} plane and {001} plane, respectively[13,14]. The activation of multiple slip systems results in dislocations intersection between different slip systems and the dislocations tangle and dislocation network form[15,16].

2.4 Discussion

Slip is the main deformation mechanism of superalloys, and the number of activated slip systems is related to temperatures. At relatively low temperatures, the activated slip systems are limited. According to the results above, the slip system of the alloy at 760 °C is mainly {111}<110> and the deformation mechanism of the alloy is mainly single slip. Slip bands along the same direction can be observed on both the surface and inside of the ruptured specimens. Meanwhile, the diffusion rate of the elements is relatively low and the activity of the atoms is relatively weak at lower temperatures. The fracture occurs along the {111} plane, which is usually observed to be the cleavage plane in the tensile fracture of single crystal superalloys[17]. Hence, the fracture surface is characterized by quasi-cleavage feature at 760 °C. At least two octahedral slip systems are activated at 850 °C, and many small quasi-cleavage planes forms on the fracture surface. It can also be seen that the normal directions of the fracture surfaces are about 50° to the stress direction at 760 and 850 °C. However, the angle between the octahedral primary slip systems and the externally applied stress axis is theoretically calculated to be about 55°[11], which is bigger than the result in our study. This may because that there are misorientation angles between the [001] orientation of the specimens and the longitudinal direction. Thus the [001] orientation of the specimen is not completely perpendicular to the externally applied stress axis.

During the process of directional solidification, single crystal superalloys are in a dendritic growth feature, which results in well-developed parallel dendritic cores and interdendritic regions. Meanwhile, there are composition segregation between the dendritic cores and interdendritic regions, as well as a small number of microcavities which forms in the interdendritic regions at the final stage of the directional solidification process[18,19]. Consequently, the strength of the interdendritic regions is lower than that of the dendrite cores at high temperatures[9,10]. In the temperature range of 980 °C to 1100 °C, dendrites characteristics exhibiting the solidification direction are observed on the fracture surface and the proportion of dendrites characteristic on the fracture surface increases with the temperature increasing. Although the dendrites morphology is macroscopically observed on the fracture surface, a dimple feature can be apparently seen on the dendrites morphology characterized fracture surface. Thus, the fracture surface displays mixed quasi-cleavage and dimple features at 980 °C, and the fracture surfaces at 1070 and 1100 °C are characterized by dimple features.

As the temperature becomes higher, more slip systems are activated during the deformation process of the alloy, including the octahedral slip and the hexahedral slip. Meanwhile, the diffusion rate of the elements is faster and the activity of the atoms is stronger than those at relatively low temperatures. Moreover, the recovery process becomes faster during the plastic deformation at high temperatures. The quasi-cleavage fracture will be less likely to occur under these circumstances. However, dimples are usually formed as the pores grow and coalesce at high temperatures, and the pores mainly stem from original microcavities in the alloy and the movement of the dislocations[20, 21]. Therefore, the fracture surfaces at high temperatures are mainly characterized by dimple features.

Prior research on the second generation single crystal superalloy DD6 has revealed that the transverse tensile deformation mechanisms and the longitudinal tensile deformation mechanisms are similar[10]. Meanwhile, the study of a third generation single crystal superalloy shows that as the temperature increases, the longitudinal tensile fracture mechanism transforms from quasi-cleavage feature at 760 °C to dimple feature at 1100 °C[7]. Although the microstructure of the transverse specimen is different from that of the longitudinal specimen, the crystal structure of the transverse specimen is the same as the longitudinal specimen. Hence, the tensile deformation mechanisms of them are similar in the temperature range of 760 °C to 1100 °C.

From the results above, we know that the transverse tensile strength decreases as the temperature increases. However, the transverse tensile elongation increases with the temperature increasing. For instance, the transverse tensile elongation at 760, 980 and 1100 °C is 9.4%, 22.5% and 29.8%, respectively. Besides, there are no apparent neck-down of the specimens near the fracture surface in the temperature range of 980 °C to 1100 °C. The neck-down of the specimens is caused by the non-uniform and localized deformation[22]. As mentioned above, more slip systems are initiated and the elements diffusion rate is relatively fast at high temperatures. Thus, the plastic deformation process of the alloy is more homogeneous, and the transverse tensile elongation is good at high temperatures.

3 Conclusions

1) At the temperatures of 760, 850, 980, 1070 and 1100 °C, the transverse tensile strength of a nickel-based third generation single crystal superalloy decreases as the temperature increases, while the transverse tensile elongation

of the alloy increases with the temperature increasing.

2) At 760 and 850 °C, the fracture surfaces of the transverse tensile ruptured specimens are characterized by quasi-cleavage features. At 980 °C, the fracture surface displays mixed quasi-cleavage and dimple features. At 1070 and 1100 °C, the fracture surfaces are characterized by dimple features.

3) At 760 °C, high density *a*/2<110> dislocations are found to be of a roughly parallel distribution with each other in the tensile ruptured specimens. The dislocations are observed to be tangled at 980 °C and dislocation networks have formed at 1100 °C.

References

1 Gell M, Duhl D N, Giamei A F. *Superalloys 1980*[C]. Warrendale: TMS, 1980: 205

2 Li J R, Liu S Z, Wang X G *et al*. *Superalloys 2016*[C]. Warrendale: TMS, 2016: 57

3 Shi Zhenxue, Liu Shizhong, Li Jiarong. *Rare Metal Materials and Engineering*[J], 2014, 43(5): 1138 (in Chinese)

4 Shah D M, Duhl D N. *Superalloys 1984*[C]. Warrendale: TMS, 1984: 105

5 Sengupta A, Putatunda S K, Bartosiewicz L *et al*. *Journal of Materials Engineering and Performance*[J], 1994, 3(1): 73

6 Li Jiarong, Shi Zhenxue, Yuan Hailong *et al*. *Journal of Materials Engineering*[J], 2008, 12: 6 (in Chinese)

7 Wang Xiaoguang, Li Jiarong, Yu Jian *et al*. *Acta Metallurgica Sinica*[J], 2015, 51(10): 1253 (in Chinese)

8 Zhang Peng, Yuan Yong, Li Bo *et al*. *Philosophical Magazine Letters*[J], 2016, 96(6): 238

9 Zhao Jinqian, Li Jiarong, Liu Shizhong *et al*. *Journal of Materials Engineering*[J], 2007, 12: 12 (in Chinese)

10 Shi Zhenxue, Li Jiarong, Liu Shizhong *et al*. *Journal of Aeronautical Materials*[J], 2009, 29(2): 101 (in Chinese)

11 Tamaki H, Fujita K, Okayama A *et al*. *Superalloys 2004*[C]. Warrendale: TMS, 2004: 145

12 Yu Xingfu, Du Hongqiang, Tian Sugui *et al*. *Rare Metal Materials and Engineering*[J], 2012, 41(12): 2185 (in Chinese)

13 Kubin L P, Lisiecki B, Caron P. *Philosophical Magazine A*[J], 1995, 71(5): 991

14 Ding Zhiping, Liu Yilun, Yin Zeyong. *Journal of Mechanical Strength*[J], 2003, 25(3): 254 (in Chinese)

15 Liu Jinlai, Yu Jinjiang, Jin Tao *et al*. *Transactions of Nonferrous Metals Society of China*[J], 2011, 21(7): 1518

16 Feller-Kniepmeier M, Link T, Poschmann I *et al*. *Acta Materialia*[J], 1996, 44(6): 2397

17 Ebrahimi F, Yanevich J, Deluca D P. *Acta Materialia*[J], 2000, 48(2): 469

18 Zhang Xiaoyue, Liu Lin, Huang Taiwen *et al*. *Rare Metal Materials and Engineering*[J], 2013, 42(12): 2547 (in Chinese)

19 Chen Q Z, Kong Y H, Jones C N *et al*. *Scripta Materialia*[J], 2004, 51(2): 155

20 Srivastava A, Gopagoni S, Needleman A *et al*. *Acta Materialia* [J], 2012, 60(16): 5697

21 Zhang X, Jin T, Zhao N R *et al*. *Materials Science and Engineering A*[J], 2008, 492(1): 364

22 Tian Lixi, Chen Jing, Xu Cong *et al*. *Materials Characterization* [J], 2016, 115: 55

一种镍基第三代单晶高温合金的横向拉伸性能

杨万鹏，李嘉荣，刘世忠，史振学，赵金乾，王效光

(北京航空材料研究院 先进高温结构材料重点实验室，北京 100095)

摘　要：在 760 ℃到 1100 ℃条件下，研究了一种镍基第 3 代单晶高温合金的横向拉伸性能。采用光学显微镜（OM）、场发射扫描电子显微镜（FESEM）与扫描透射电子显微镜（STEM）观察了合金的显微组织与断口形貌。结果表明：随着温度的升高，合金的抗拉伸强度降低，而拉伸延伸率增加。在 760 与 850 ℃条件下的拉伸断裂均为类解理断裂。在 980，1070 和 1100 ℃条件下，试样断口出现了反映凝固方向的枝晶形貌特征，且随着温度的升高枝晶形貌在断口上的面积增加。在 980 ℃条件下，拉伸断裂为类解理断裂与韧窝断裂的混合断裂。在 1070 和 1100 ℃条件下，拉伸断裂均为韧窝断裂。随着温度的升高，塑性变形过程中开动了更多滑移系，导致形成了不同的位错形貌。760 ℃拉伸，合金中出现了高密度大致平行分布的 *a*/2<110>位错；980 ℃拉伸，合金中出现了位错缠结；1100 ℃拉伸，合金中形成了位错网络。

关键词：第 3 代单晶高温合金；横向拉伸性能；断口；位错

作者简介：杨万鹏，男，1988 年生，博士生，北京航空材料研究院先进高温结构材料重点实验室，北京 100095，电话：010-62498312，E-mail: wp_yang621@126.com